

Research Article

Ultrasonic Functionalized Egg Shell Powder for the Adsorption of Cationic Dye: Equilibrium and Kinetic Studies

Veluru Sridevi ¹, B. Senthil Rathi ², P. Senthil Kumar ^{3,4}, A. Saravanan ⁵,
R. V. Hemavathy ⁶, S. Karishma ⁶, S. Jeevanantham ⁶, Sri Himaja Pamu ¹,
Lam Sudha Rani ¹ and K. S. N. V. Prasad ¹

¹Department of Chemical Engineering, AU College of Engineering, Andhra University, 530003, Visakhapatnam, Andhra Pradesh, India

²Department of Chemical Engineering, St. Joseph's College of Engineering, Chennai 600119, India

³Department of Chemical Engineering, Sri Sivasubramaniya Nadar College of Engineering, Chennai 603110, India

⁴Centre of Excellence in Water Research (CEWAR), Sri Sivasubramaniya Nadar College of Engineering, Chennai 603110, India

⁵Department of Energy and Environmental Engineering, Saveetha School of Engineering, SIMATS, 602105, Chennai, India

⁶Department of Biotechnology, Rajalakshmi Engineering College, 602105, Chennai, India

Correspondence should be addressed to B. Senthil Rathi; rathisjce@gmail.com and P. Senthil Kumar; senthilkumarp@ssn.edu.in

Received 8 February 2022; Revised 17 March 2022; Accepted 5 April 2022; Published 22 April 2022

Academic Editor: Muhammad Raziq Rahimi Kooh

Copyright © 2022 Veluru Sridevi et al. This is an open access article distributed under the Creative Commons Attribution License, which permits unrestricted use, distribution, and reproduction in any medium, provided the original work is properly cited.

The present research focuses on synthesizing surface-modified egg shell powders using ultrasonic modification method for the effective adsorption of malachite green dye (MG). The presence of functional groups and surface morphology of ultrasonic-assisted egg shell powder (UAESP) was characterized using Fourier transform infrared spectrophotometer (FTIR) and scanning electron microscopy (SEM) analysis, respectively. A batch adsorption study was performed to predict the optimum conditions, and the results showed that maximum adsorption rate at the solution pH of 8.0 within the interaction time of 90 min, dosage of 1.5 g/L for MG dye concentration of 25 mg/L, and temperature 30°C. The isotherm and kinetics modeling of the present adsorption system can be well described by Freundlich and pseudosecond-order kinetics, respectively. The monolayer adsorption capacity of UAESP for MG dye was originated to be 64.58 mg/g. The results of the thermodynamic study reported that adsorption removal of MG dye onto UAESP was exothermic and spontaneous. This study accredited that UAESP has higher efficiency, cost-effective, and sustainable adsorbent for the removal of hazardous dyes on an industrial level.

1. Introduction

Environmental pollution, a global phenomenon, is greatly exacerbated by industrialization and urbanization with its deleterious implications on all organisms. Water pollution and land pollution have risen in recent years due to the introduction of excess effluent amount into the environment. Unmet needs for improved water availability have compelled industrialists to concentrate on treatment technologies. Untreated industrial effluent causes water quality to stagnate, threatening the lives of many organisms [1]. The dye effluent is extremely hazardous as it comprises a large number of suspended solids, chemicals, COD, dye,

and heavy metals. Dye, as a visible pollutant, is highly undesirable even in trace amounts [2–4]. Dyes are organic compounds consisting of two main groups of compounds, chromophores (responsible for the color of the dye), and auxochromes (responsible for the intensity of the color). The colorants in textile dyes prevent sunlight from probing water, slowing the rate of oxygen uptake, and photosynthesis. Aside from persisting as environmental pollutants, they also act as cancer-causing, mutagenic, and lethal agents, passing contaminants up the food chain from lower to higher trophic levels [5, 6]. The color of the dye interrupts the normal aesthetic life of marine organisms. MG dye, an N-methylated diaminotriphenyl methane basic dye, is

perhaps the most prevalently utilized dye in the textile, wool, and leather industries [7]. The noxious and metal chelating nature of MG dye harms the internal organs of organisms ranging in trophic levels from medium to higher. In its reduced form—leucomalachite green—MG dye acts as an apoptotic agent as well as a tumor promoter [8, 9].

To treat dye-polluted water, conventional methods including membrane separation, magnetic separation, advanced oxidation processes, photocatalysis, reverse osmosis, coagulation, adsorption, and ion exchange have been used. Each degree has a varying level of success. The use of environmentally and economically sustainable materials has made adsorption, a viable and suitable wastewater treatment process [10–13]. Adsorption to date is the most effective and utilized technology globally to remove several pollutants in wastewater. However, there are many challenges to adsorption processes such as reducing the high cost, through means of separation of suspending adsorbents to be used again, as well as the ease to synthesize [14]. On the other hand, adsorbents have a synergistic effect with their efficient adsorption capacity to remove contaminants, high abundance, and participation in waste minimization, helping alleviate ecological and environmental problems [15].

Additionally, biobased adsorbent materials such as agricultural, animal, and plant wastes outperform synthetic adsorbents. Carbon-based compounds with high superficial properties and sorption abilities adsorb more adsorbate onto adsorbents [16]. Commonly employed adsorbents for removal of malachite green dye include sugarcane composite [17], *Livistona chinensis* [18], *Artocarpus odoratissimus* biochar [19], *Coriolus versicolor* [20], *Limonia acidissima*—wood apple shell [21], and *Pinus roxburghii* cone adsorbent [22].

In the majority of developing countries, solid residues such as animal waste are dumped into the ground, causing harmful effects on organisms. Crab shells, fish bones, chicken bones, egg shells, and other animal wastes are examples of animal residues. Egg shell is opulent animal waste that is recycled in a limited range. Every year, millions of egg shells are discarded as waste in the country without being recycled [23–25]. Egg shells are a significant source of waste in the chicken egg processing industry. As a natural calcium carbonate source with other trace elements, it can be used as a dye sorbent. Customarily, chemically synthesized calcium carbonate was used in the pollutant removal process. Although the calcium carbonate in egg shells is not as pure as a chemical reagent, it can be used effectively in the adsorption process. Cockle shell, chicken bones [26], cuttle fish bone waste [27], mussel shell [28], and *Labeo rohita* fish scale wastes [29] are examples of recent animal waste-based adsorbents used in pollutant remediation.

Activated carbon has better prospects in adsorption applications. The conventional adsorbent materials can be modified to activated carbon with better porosity and surface area. In the physical methods, material is carbonized in oxygen absence. Fixed concentrations of activating reagents are added to eliminate the moisture content and modify the chemical properties of the adsorbent materials [30, 31]. The reduced requirement inactivation procedure has made the ultrasound technique a better process. The

pressure waves in the medium generate the ultrasound waves leading to modification. Negative pressure exists when the acoustic pressure amplitude exceeds the static pressure. Negative pressure in the solid-liquid aqueous system causes molecular expansion. It also breaks the molecular bond creating cavities and pores. For material activation, a frequency of 35 kHz is preferable [32–34]. Many recent adsorption studies have used reactive adsorbents such as ultrasonicated dragon fruit peel biomass [35], ultrasound pretreated peanut husk powder [36], and ultrasonication modified corn-pith [37]. As ultrasonically treated shells have not been used previously, the ultrasonicated egg shell powder is being investigated in this study for malachite green dye adsorption.

In the present research, UAESP is utilized as an adsorbent for the sorption of MG dye from synthetic solutions. To depict the properties of the modified adsorbent, scanning electron microscopy (SEM) and Fourier transform infrared (FTIR) were used. By utilizing UAESP, batch experimental studies were carried out using the various variables for instance time, pH, temperature, the dose of UAESP, and initial concentration of MG dye. The adsorption equilibrium data were applied to isotherm and kinetic modeling study to determine the mechanism of MG dye sorption onto ultrasonicated egg shell powder. The influence of temperature on the sorption framework was predicted by scrutinizing thermodynamic experiments.

2. Experimental Study

2.1. Adsorbate. Malachite green, a cationic dye, was acquired from E. Merck in Bangkok, Thailand, and included as an adsorbate in the current study. 1 liter of standard MG dye aqueous solution was obtained by dispersing 1 g of dye in 1 liter of distilled water. Dilutions of the standard typically result from in-stock solutions with concentrations extending from 25 mg/L to 150 mg/L. The dye concentration was assessed using ultraviolet-visible spectroscopy at 620 nm.

2.2. Synthesis and Characterization—UAESP. Egg shells were collected and cleansed thoroughly in distilled water several times to eliminate impurities. After that, the shells were dried, crushed, and ground into a fine powder. The powdered egg shells were sieved until the particle size was less than 74 microns. A known quantity of derived powder is mixed with a known volume of distilled water. The sample was modified using an ultrasonication process. In an ultrasonicator (Sonic Materials Inc., Newtown, USA) to 500 rpm and 24 kHz frequency, the solution mixture was agitated for 1 hour. The sonicated mixture was filtered and dried for 12 hours at 50°C. The resultant modified adsorbent powder was termed ultrasonic-activated egg shell powder (UAESP). The schematic diagram for the preparation of UAESP was shown in Figure 1. FTIR (Perkin Elmer, FTIR C100566, UK) analysis from 400 to 4000 cm^{-1} in ATR (Attenuated Total Reflectance) mode was applied to investigate the superficial functional moieties of UAESP. Scanning electron microscopy (SEM) (Phenom-World BV, Eindhoven, Netherlands) has also been used to examine the morphology of the sample before and after adsorption.

2.3. Batch Experimental Studies. To check the coherence of parameters influencing the adsorption process such as adsorbent dosage (0.25–2 g/L), solution pH (2.0–10.0), concentration of MG dye (25–150 mg/L), period (10–120 min), and process temperature (303–333 K), a notable quantity of prepared adsorbent is blended with desired concentrations of aqueous MG dye solutions. Then, the mixture was left for agitation in a shaker at 300 rpm speed, and other parameters were kept constant. A known amount of samples was drawn out at regular time interludes, centrifuged, and analyzed for leftover dye concentration by UV spectroscopy analysis.

$$\% \text{removal of MG dye} = \frac{(C_i - C_f)}{C_i} \times 100, \quad (1)$$

where C_i and C_f mean the concentration of MG dye (mg/L) before and after adsorption.

2.4. Experimental Study of Isotherm Plot. For the analysis of isotherm, experiments with MG dye concentrations (25–150 mg/L) with a known adsorbent dosage (1.5 g/L) were performed at a consistent temperature (303 K) and pH (8) in a shaking incubator. Following the preordained time, spent adsorbent was retrieved from the adsorption solutions by centrifugation at 4000 rpm for 15 min. Using UV spectroscopy analysis, analysis of supernatant for dye concentration was executed. The adsorbent adsorption capacity at equilibrium was determined by the equation

$$q_e = \frac{(C_i - C_e)V}{m}. \quad (2)$$

Here, q_e signifies the equilibrium adsorption ability (mg/g) and m and V are the mass of adsorbent (mg) and MG dye solution volume (L).

The data from isotherm experiments would be fitting with Freundlich, Langmuir, Temkin, and Sips model, and parameter values were evaluated by fitting those isotherm curves by MATLAB R2020a software. The isotherm equations are as follows:

Langmuir model [38]:

$$q_e = \frac{q_m K_L C_e}{1 + K_L C_e}. \quad (3)$$

Here, q_m , K_L , and q_e denote Langmuir maximum adsorption ability (mg/g), energy constant of Langmuir isotherm, and MG dye adsorbed per unit UAESP quantity (mg/g).

Freundlich isotherm [39]:

$$q_e = K_F C_e^{1/2}. \quad (4)$$

K_F and n denote Freundlich constant (L/g) and its exponent.

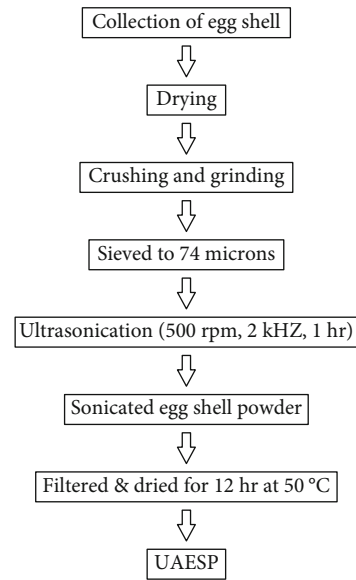


FIGURE 1: Schematic diagram for the preparation of UAESP.

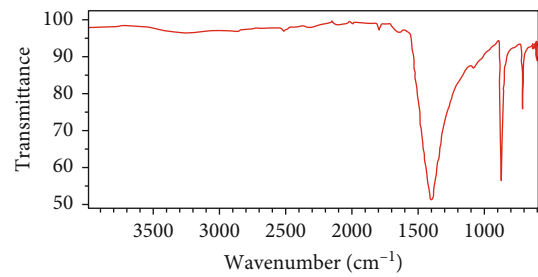


FIGURE 2: FTIR study of UAESP.

Sips model [40]:

$$q_e = \frac{K_s C_e^{\beta_s}}{1 + \alpha_s C_e^{1/\beta_s}}, \quad (5)$$

where K_s notes the adsorption capability of Sips isotherm (mg/g) and β_s denotes the Sips isotherm model exponent.

Temkin isotherm [41]:

$$q_e = \frac{RT}{b} (\ln AC_e). \quad (6)$$

Temkin isotherm constants are denoted by A and b .

2.5. Experimental Study of Kinetic Plot. Adsorption kinetic studies can guesstimate the mechanism and rate of the adsorption process. At time intervals ranging from 10 to 120 min, the kinetic experiments were performed out under optimal parameter conditions. In a shaking incubator, the samples were agitated for varying amounts of time. The supernatant was recovered through repeated centrifugation, and the remnant absorbance was recorded using

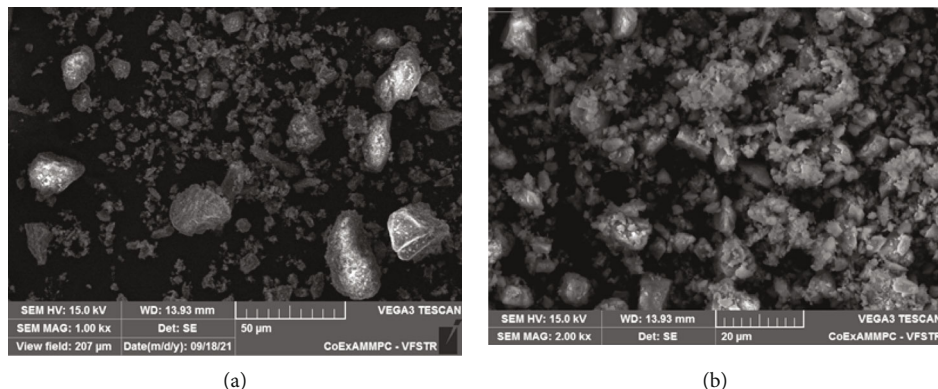


FIGURE 3: (a) SEM analysis—before adsorption. (b) SEM analysis—after adsorption.

spectrophotometry. The removal efficacy can be calculated on the basis:

$$q_t = \frac{(C_i - C_t)V}{m} \quad (7)$$

C_t and q_t represent the concentration of MG dye at a specified time “ t ” and the amount of MG dye adsorbed per unit quantity of UAESP.

Pseudofirst-order kinetics [42], pseudosecond-order kinetics [43], and Elovich kinetics [44] are represented by following equations:

$$q_t = q_e(1 - \exp(-k_1 t)), \quad (8)$$

$$q_t = \frac{(q_e^2 k_2 t)}{(1 + q_e k_2 t)}, \quad (9)$$

$$q_t = (1 + \beta_E) \ln(1 + \alpha_E \beta_E t). \quad (10)$$

Rate constant of pseudofirst-order and pseudosecond-order rate constant is denoted by k_1 and k_2 , respectively. Then, α_E denotes the desorption constant (g/mg), and β_E denotes adsorption rate (mg/g min).

2.6. Thermodynamic Studies. The nature and energy changes in MG dye adsorption by UAESP can be projected by experiments conducted at diverse temperatures extending from 303 to 333 K. The results of these experiments are used to calculate the parameters for instance ΔH^0 , ΔS^0 , and ΔG^0 by equations:

$$\Delta G^\circ = -RT \ln K_c, \quad (11)$$

$$K_c = \frac{C_{Ae}}{C_e}, \quad (12)$$

$$\text{Log}K_c = \frac{DS^\circ}{2.303R} - \frac{DH^\circ}{2.303RT}, \quad (13)$$

where C_{Ae} , R , K_c , and T represent MG dye adsorbed onto UAESP (mg/L), universal gas constant (8.314 J/Kmol), constant of equilibrium, and temperature (K).

3. Experimental Outcomes

3.1. Characterization of Ultrasonicated Adsorbent. The FTIR results interpret the existence of functional moieties on the exterior of the UAESP. Figure 2 shows the FTIR results of UAESP. Peak values at 2513 and 1794 cm^{-1} reveal the occurrence of aldehyde and carbonyl groups in the UAESP. The peaks at 1394 and 1083 cm^{-1} allow the identification of other functional groups such as phenol (O-H bend) and primary amines with C-N stretch. A sharp 871 cm^{-1} peak indicates C-O-O stretching in peroxides, and an absorption peak at 711 cm^{-1} predicts O-H out-of-plane bend. In particular, FTIR analysis reveals the alcoholic, amino, phenolic, and peroxide moieties in UAESP biomass. The inclusion of more negatively charged groups in UAESP may form interlinkages with positively charged malachite green dye, allowing for easier removal from aqueous solutions.

Figures 3(a) and 3(b) illustrate the SEM characterization of UAESP (ultrasonic-assisted egg shell powder) before and after the MG dye adsorption process (b). Micrographic images of UAESP reveal voids or spaces with conglomerated masses. Before adsorption, the UAESP surface has porous structures with uniform particle distribution and a smooth surface. Following the MG dye adsorption method, micrographs show numerous rough grooves on the adsorbent surface, as well as the perishing of pores on the exterior of UAESP. The before and after adsorption process results show the alteration of porous structures in UAESP by MG dye. Because the adsorption process is primarily determined by surface characteristics, SEM characterization confirms MG dye adsorption onto UAESP.

3.2. Impact of Parameters on MG Dye Adsorption

3.2.1. Adsorption Dosage. The percentage removal of MG dye from studies performed with a dose of UAESP extending from 0.25 to 2.0 g/L is depicted in Figure 4(a). UAESP dosage was escalated from 0.25 to 1.5 g/L; the removal percentage elevated because of constant accumulation of binding locates by MG dye. The same removal was noticed after a dosage of 1.5 g/L because of the overload of active locales on the UAESP locates. Furthermore, the obscene quantity of adsorbent to limited adsorbate, MG dye concentration,

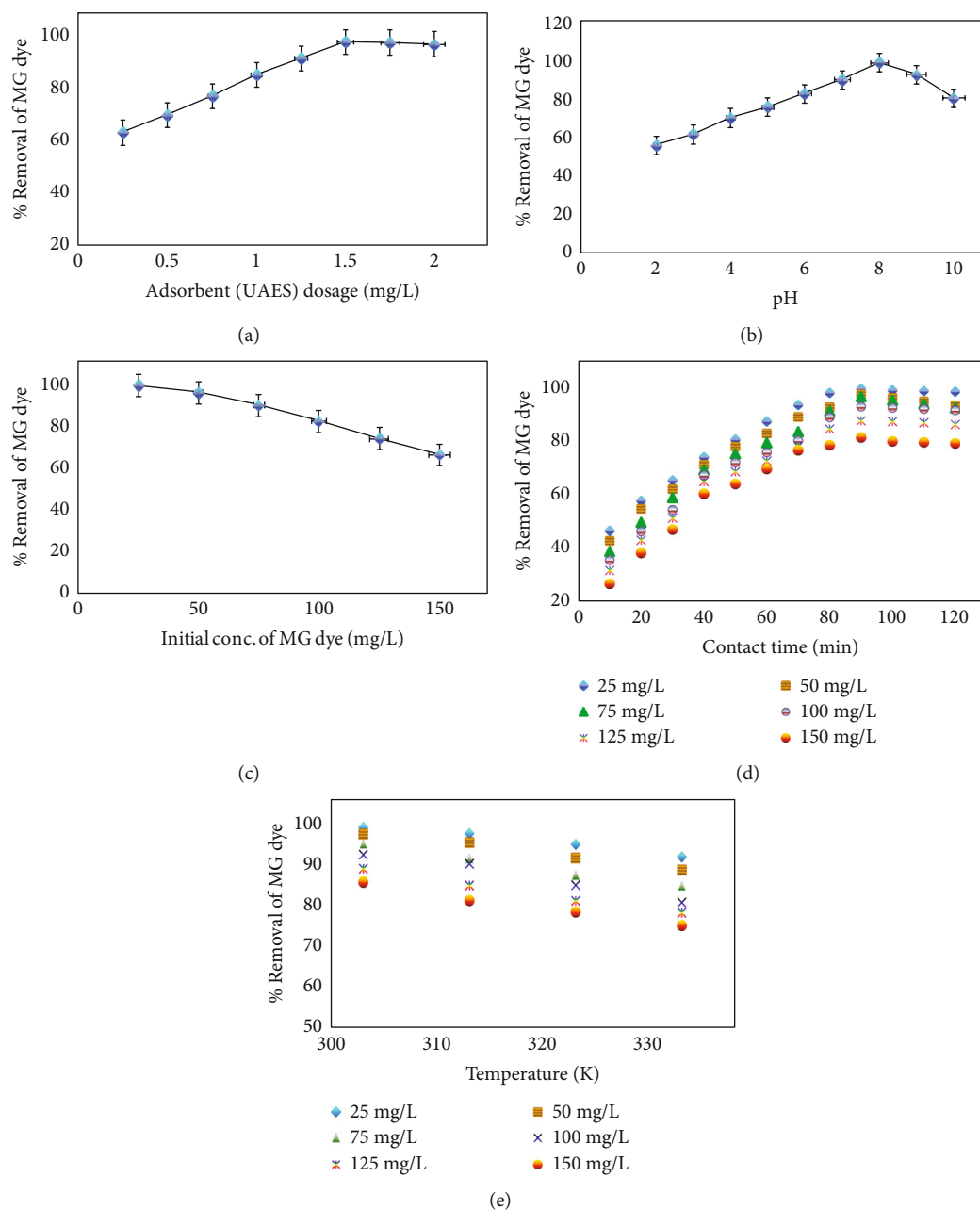


FIGURE 4: (a) Impact of adsorbent (UAESP) dosage on MG dye adsorption. (b) Impact of solution pH on MG dye adsorption. (c) Impact of Initial MG dye concentration on MG dye adsorption. (d) Influence of contact time on the adsorption of MG dye. (e) Influence of Temperature on the adsorption of MG dye.

and the assemblage of locates, are the reasons for reduced removal. For practical applications, the adsorbent dosage must be fixed for larger effluent volumes. According to the findings of this study, optimal UAESP dosage of 1.5 g/L is effective in removing MG dye from aqueous solutions.

3.2.2. pH. The surface properties of the adsorbent can be altered by pH, which is a significant factor in the adsorption process. Experiments with pH ranging from 2.0 to 10.0 were performed to estimate the pH effect on MG dye sorption, as shown in Figure 4(b). The figure shows that MG dye sorption improved with pH values extending from 2.0 to 8.0.

The high reliance of MG sorption on functional group protonation and deprotonation makes the process more compatible with a suitable pH. Electrostatic interaction between UAESP and MG dye molecules at alkaline pH range due to the influence of highly negatively charged molecules. Because of MG dye hydrolysis above that pH, the pH value of 8.0 was optimal.

The pH at which the sorbent surface charge takes a zero value is defined as the point of zero charge (pHpzc). At this pH, the charge of the positive surface sites is equal to that of the negative ones. The knowledge of pHpzc allows one to hypothesize on the ionization of functional groups and their

TABLE 1: Isotherm parameters and their goodness of fit for MG dye adsorption onto ultrasonic-assisted egg shell (UAESP).

S. no.	Models	Parameters			R^2	SSE	RMSE
1	Langmuir	$q_m(\text{mg/g})$ 64.58	$K_L(\text{L/mg})$ 0.4104		0.9331	2.19	5.454
2	Freundlich	$n(\text{g/L})$ 3.974	$K_F((\text{mg/g}) (\text{L/mg})^{(1/n)})$ 20.19		0.9919	1.04	1.97
3	Temkin	$A_T(\text{L/g})$ 3.9	$B(\text{J/Mol})$ 5.544		0.9052	2.68	5.805
4	Sips	$K_s(\text{L/g})$ 25.28	α_s 5.033	β_s 0.2514	0.9881	1.15	2.299

interaction with dye species in solution; at solution pHs higher than pH_{pzc} , sorbent surface is negatively charged and could interact with dye positive species, while at pH slower than pH_{pzc} , solid surface is positively charged and could interact with negative species.

3.2.3. Concentration of MG Dye. To find the impact of the concentration of MG dye on sorption, studies with varied ranges of 25 to 150 mg/L were carried out, as shown in Figure 4(c). At high MG dye concentrations, instantaneous saturation of MG dye molecules on the UAESP surface resulted in a lower percentage removal. Even though the dye concentration increases, the fixed UAESP dosage has a limited number of active locations. When the adsorbent-to-dye dosage ratio is low, high energy sites are saturated, and removal decreases due to low energy adsorption sites. Moreover, at high concentrations, mass transfer resistance between UAESP and MG dye molecules induces the resistance driving force, which influences the process. UAESP detected maximum sorption at an MG concentration of 25 mg/L.

3.2.4. Contact Time. At an adsorbent dosage of 1.5 g/L, the concentration of MG -25 mg/L, and a solution pH of 8.0, the impact of contact time was investigated over 10 minutes to 120 minutes, the results of which are shown in Figure 4(d). The increased likelihood of dye molecule collision with UAESP surface improves the sorption process. Also, the adsorption process continues until the system attains equilibrium. As a result, adsorption was rapid, and after 90 minutes, removal was at its peak and remained consistent. Because the exterior located on the UAESP surfaces are completely engaged by MG dye molecules. This process is also aided by fewer adsorbent sites and a higher dye concentration. In subsequent time intervals, adsorbent molecules repel each other, slowing the adsorption process. The operation time of 90 min is ideal for current MG dye adsorption by UAESP.

3.2.5. Temperature. The impact of temperature on MG adsorption onto UAESP is displayed in Figure 4(e). With increased temperature, the removal percentage of MG dye was originated to decrease. At higher temperatures, the superficial activity of the adsorbent decreases. Also, adsorbent requires more energy to be stable in a liquid medium

for a prolonged period which alters the balance in the sorption technique. The vapor pressure in the adsorption system raises, and adsorbent density gradually diminishes that also affects the biosorption process. This result signifies the exothermic nature and low-temperature favourness of adsorption system. The highest percentage removal of MG dye was experimental at a temperature of 303 K.

3.3. Isotherm Modeling. Adsorption isotherm models are critical in ascertaining the mechanism of interaction of UAESP with MG dye and the sorption capability of UAESP. The correlation of equilibrium curves is critical in the design of improved and optimised adsorption systems. Table 1 summarises the values of isotherm parameters and their corresponding goodness of fit obtained from the studies. Figure 5(a) illustrates the isotherm fit for MG dye adsorption onto UAESP.

The adsorption mechanism is likely to be electrostatic interaction between negatively charged surface and the cationic dye molecules. Adsorption isotherm gives us valuable information regarding the adsorbate-adsorbent interaction. A few of the most common isotherms models like Freundlich isotherm, Langmuir isotherm, and Temkin isotherm are developed by taking into consideration the effects of adsorbate-adsorbent interactions, and it is based on the assumption that heat of adsorption of all molecules in the layer decreases linearly as surface coverage increases. The increase in initial dye concentration equals the increase in the total amount of dye molecules in the fixed solution volume and adsorbent mass. Thus, more adsorbates could bind to the active sites on the adsorbent at higher dye concentration, resulting in higher adsorption capacities.

The Langmuir isotherm, which describes the homogeneous adsorption system, does not provide the best fitting results for the current study. The Langmuir isotherm's monolayer adsorption ability was estimated to be 64.58 mg/g. The Temkin model, which assumes a larger surface coverage area with linear adsorption heat diminishment, also did not fit the current system. It is applicable at higher adsorbate concentrations in the case of the sips isotherm. At lower bioadsorbate concentrations, the Freundlich equation can be used instead of the sips isotherm. The Freundlich isotherm model, which describes the multilayer interaction of adsorbent with sorbate molecules, applies to surfaces with heterogeneous distribution. Higher R^2 values ($R^2=0.9919$)

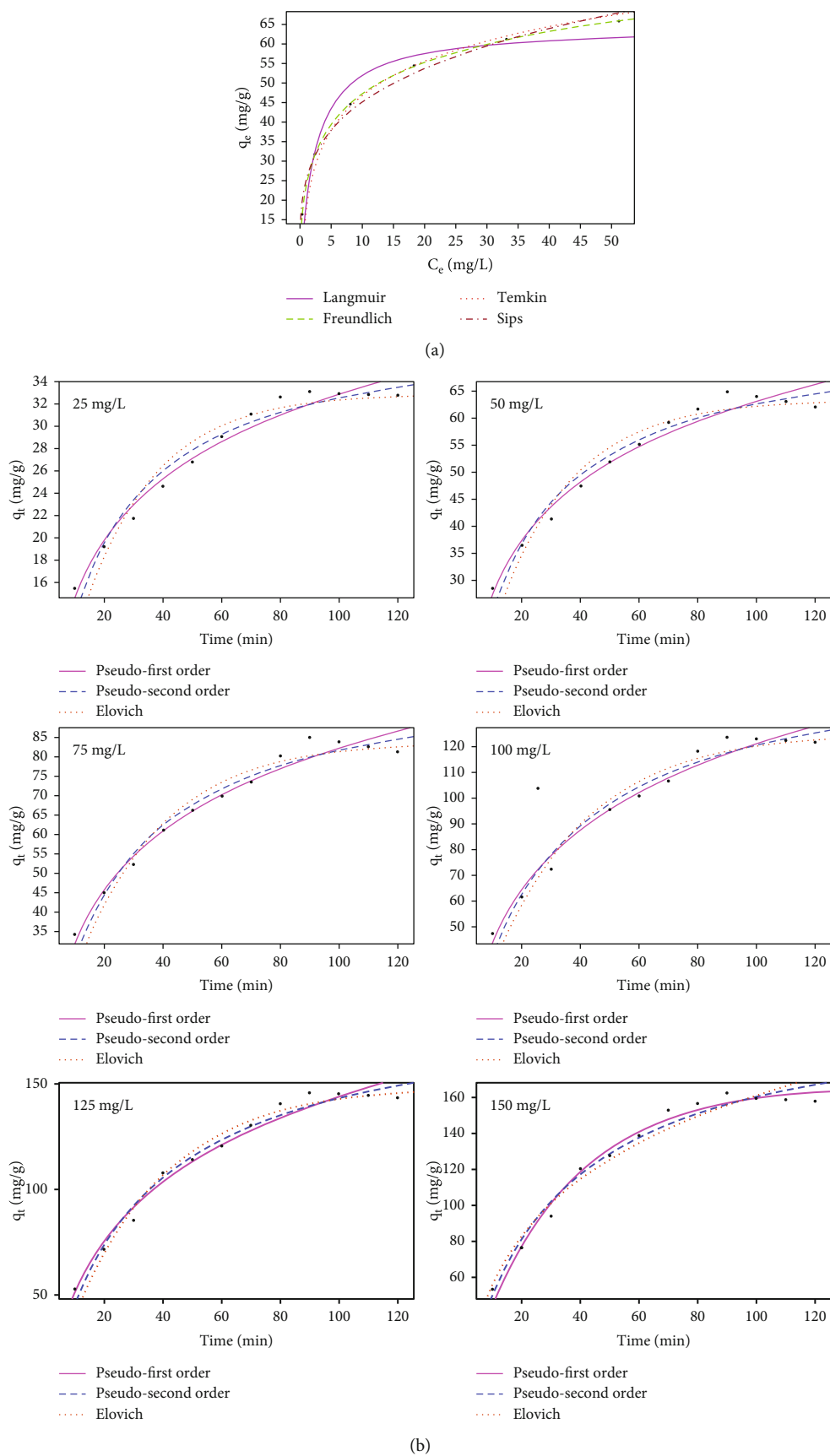


FIGURE 5: Continued.

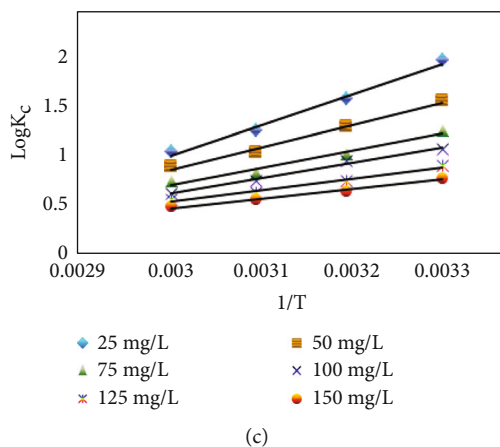


FIGURE 5: (a) Isotherm fit for the adsorption of MG dye onto UAES. (b) Kinetic fit for the adsorption of MG dye onto UAES. (c) Thermodynamic study for the adsorption of MG dye onto UAES.

TABLE 2: Assessment of q_m value of UAESP with the previously used materials for MG dye adsorption.

S. no.	Adsorbent	Optimum conditions			Best fitted model	Adsorption capacity (q_m) (mg/g)	References
		Time (min)	Dosage (g/L)	Temperature (K)			
1	CNF aerogel	40	2.5	—	Langmuir	212.7	[45]
2	Opuntia ficusindica	120	4.0	298	Langmuir	200.1	[46]
3	Wood apple shell (WAS)	210	0.05	299	Langmuir	80.645	[21]
4	Ultrasonic-assisted egg shell powder (UAESP)	90	1.5	303	Freundlich	64.58	This study
5	Functionalized Zea Mays Cob (FZMC)	120	—	298	Freundlich	64.52	[47]
6	<i>Zingiber officinale</i> (ginger) leaves	120	0.4	—	Langmuir	48.91	[48]
7	Sulfur-treated tapioca peel biochar	120	2.0	—	Langmuir	30.18	[49]
8	Cd(OH) ₂ -NW-AC	50	0.6	298	Langmuir	19.0	[50]
9	Chitosan-ZnO composite	180	6.0	293	Langmuir	11.0	[51]
10	<i>Pinus patula</i> biochar	60	6.0	—	—	9.8	[52]
11	Brewers' spent grain (BSG)	20	6.0	296	Langmuir	2.55	[53]

TABLE 3: Kinetics parameters for MG dye adsorption onto UAESP.

S. no.	Models	Parameters	Initial MG dye concentration (mg/L)					
			25	50	75	100	125	150
1	Pseudofirst order	$q_e(\text{exp})$	32.86	62.59	82.38	123.97	145.64	161.25
		$q_e(\text{mg/g})$	32.91	63.43	83.97	125.5	149.1	166.9
		$k_1(\text{min}^{-1})$	0.0408	0.0396	0.0348	0.0316	0.0315	0.0312
		R^2	0.971	0.9696	0.9723	0.9772	0.9759	0.9829
2	Pseudosecond order	$q_e(\text{mg/g})$	39.18	76.04	103.1	157	187.7	212
		$k_2(\text{g/mg min})$	0.0013	0.0006	0.0004	0.0002	0.0002	0.0001
		R^2	0.9596	0.9636	0.9678	0.9729	0.9695	0.9763
3	Elovich	α_E	0.1666	0.0628	0.0276	0.0126	0.0096	0.0074
		β_E	2.722	6.385	9.74	16.18	19.85	23.13
		R^2	0.92	0.9324	0.9467	0.9568	0.9624	0.9617

TABLE 4: Thermodynamic parameters for the adsorption of MG dye onto UAESP.

S. no.	Parameters	Temperature (K)	Initial MG dye concentration (mg/L)					
			25	50	75	100	125	150
1	ΔG° (KJ/Mol)	303	-11.5005	-9.0492	-7.3494	-6.25	-5.2311	-4.4985
		313	-9.4913	-7.8026	-6.1044	-5.7352	-4.4483	-3.8039
		323	-7.8125	-6.3709	-5.1744	-4.6413	-3.9096	-3.4603
		333	-6.6654	-5.6579	-4.7399	-3.959	-3.5316	-3.0519
2	ΔH° (KJ/Mol)		-60.6869	-44.3429	-34.0226	-30.4133	-22.4787	-18.7163
3	ΔS° (J/Mol/K)		-162.942	-116.734	-88.6168	-79.4549	-57.1963	-47.2073

and lower error values (SSE—1.04 and RMSE—1.97) of experimental data were in better agreement with the Freundlich isotherm. In general, K_F values indicate the sorption capacity of an adsorbent. Higher K_F values in this context represent the greater multilayer sorption ability of the synthesised novel adsorbent—UAESP. The value $n = 3.974$, which is greater than one, indicates that the physical nature of the sorption technique is favorable. The capacity of UAESP adsorbent with other previous adsorbents was compared and shown in Table 2. It inferred better bioadsorption capacity relative to most adsorbents.

3.4. Kinetic Modeling. The rate of adsorbent UAESP uptake and the residence time of adsorption can be predicted by kinetic investigation. Statistical parameters of the kinetic were acquired from experiments and are represented in Table 3. The kinetic fit for MG dye adsorption onto UAESP was shown in Figure 5(b). From the investigation, kinetics of MG dye removal by UAESP represented the finest fitting with pseudosecond order. The model parameters R^2 value was greater with pseudofirst-order kinetics compared to other models. The experimental value of adsorption ability q_e was originated to be in adjacent correlation with theoretical q_e value in case pseudofirst-order kinetics. This explicates the physically controlled nature of adsorption process. Also, the rate of sorption process diminishes with high concentration of MG dye owing to its high binding site competition in the UAESP surface, and low concentration avails the maximum active sites for MG molecules to bind. The preference of hydrogen bonds with van der Waals forces was evident from physical attributes of current MG dye sorption.

3.5. Thermodynamic Study. Thermodynamic parameters are also significant in assessing the adsorption mechanism of the current system. The thermodynamic variables—enthalpy and entropy alteration (ΔH° and ΔS°)—were calculated using a plot between $\log Kc$ and $1/T$, as shown in Figure 5(c). Table 4 shows the experimentally determined thermodynamic study parameters. The presence of exothermic properties in the MG dye adsorption process is inferred by the negative ΔH° values. As the adsorbate becomes trapped on the surface of the UAESP, the randomness and movement of molecules in the solid-liquid interface system decreases, resulting in negative entropy (ΔS°) values. The reduced change in Gibb's free energy values with increasing temperature confirms the process's feasibility and spontane-

ity. Furthermore, the ΔG° values range from -20 to 0 kJ/mol, explaining the physisorption MG dye removal process. Precisely, the exothermic, physisorption, feasibility, and spontaneity of MG dye adsorption onto UAESP have been interpreted from thermodynamic experiments.

4. Conclusion

In this research study, ultrasonically activated egg shell powder has been investigated for its adsorption properties for MG dye removal. The characterization analysis—SEM and FTIR—revealed that ultrasonic-activated egg shell powder has better porous properties and groups. Batch experiments revealed that optimal adsorption occurred at a solution pH of 8.0, a UAESP dosage of 1.5 g/L for a concentration of MG dye -25 mg/L, a temperature of 30°C, and an interaction time of 90 minutes. Pseudosecond-order and Freundlich model best designate the kinetics and isotherm of the adsorption system. Thermodynamic conducts disclose the process's spontaneous and exothermic nature. As a result, ultrasonic-activated egg shell powder is a low-cost and effective adsorbent for dye removal from synthetic solutions.

Data Availability

Data are available on request.

Conflicts of Interest

The authors declare that they have no conflicts of interest.

References

- [1] A. A. Beni and A. Esmaeili, "Biosorption, an efficient method for removing heavy metals from industrial effluents: a review," *Environmental Technology and Innovation*, vol. 17, article 100503, 2020.
- [2] B. Bharathiraja, I. A. B. Selvakumari, J. Iyyappan, and S. Varjani, "Itaconic acid: an effective sorbent for removal of pollutants from dye industry effluents," *Current Opinion in Environmental Science & Health*, vol. 12, pp. 6–17, 2019.
- [3] B. Lellis, C. Z. Favaro-Polonia, J. A. Pamphile, and J. C. Polonia, "Effects of textile dyes on health and the environment and bioremediation potential of living organisms," *Biotechnology Research and Innovation*, vol. 3, no. 2, pp. 275–290, 2019.
- [4] A. Saravanan, S. Karishma, S. Jeevanantham et al., "Optimization and modeling of reactive yellow adsorption by surface modified *Delonix regia* seed : study of nonlinear isotherm

- and kinetic parameters,” *Surfaces and Interfaces*, vol. 20, article 100520, 2020.
- [5] F. R. Abe, A. L. Machado, A. M. V. M. Soares, D. P. Oliveira, and J. L. T. Pestana, “Life history and behavior effects of synthetic and natural dyes on *Daphnia magna*,” *Chemosphere*, vol. 236, article 124390, 2019.
 - [6] V. Katheresan, J. Kansedo, and S. Y. Lau, “Efficiency of various recent wastewater dye removal methods: a review,” *Journal of Environmental Chemical Engineering*, vol. 6, no. 4, pp. 4676–4697, 2018.
 - [7] N. Kumar, H. Mittal, S. M. Alhassan, and S. S. Ray, “Bionano-composite hydrogel for the adsorption of dye and reusability of generated waste for the photodegradation of ciprofloxacin: a demonstration of the circularity concept for water purification,” *ACS Sustainable Chemistry & Engineering*, vol. 6, no. 12, pp. 17011–17025, 2018.
 - [8] T. A. Ferreira, I. S. Ibarra, M. L. S. Silva, J. M. Miranda, and J. A. Rodriguez, “Use of modified henequen fibers for the analysis of malachite green and leuco-malachite green in fish muscle by d-SPE followed by capillary electrophoresis,” *Microchemical Journal*, vol. 157, article 104941, 2020.
 - [9] T. R. Sundararaman, A. Saravanan, P. Senthil Kumar et al., “Adsorptive removal of malachite green dye onto coal-associated soil and conditions optimization,” *Adsorption Science and Technology*, vol. 2021, article 5545683, pp. 1–11, 2021.
 - [10] E. Brillas, “Recent development of electrochemical advanced oxidation of herbicides. A review on its application to wastewater treatment and soil remediation,” *Journal of Cleaner Production*, vol. 290, article 125841, 2021.
 - [11] S. Samsami, M. Mohamadizani, M.-H. Sarrafzadeh, E. R. Rene, and M. Firoozbahr, “Recent advances in the treatment of dye-containing wastewater from textile industries: overview and perspectives,” *Process Safety and Environment Protection*, vol. 143, pp. 138–163, 2020.
 - [12] S. H. Teo, C. H. Ng, A. Islam et al., “Sustainable toxic dyes removal with advanced materials for clean water production: a comprehensive review,” *Journal of Cleaner Production*, vol. 332, article 130039, 2022.
 - [13] K. Vikrant, B. S. Giri, N. Raza et al., “Recent advancements in bioremediation of dye: current status and challenges,” *Biore-source Technology*, vol. 253, pp. 355–367, 2018.
 - [14] S. Maswanganyi, R. Gusain, N. Kumar, E. Fosso-Kankeu, F. B. Waanders, and S. S. Ray, “Bismuth molybdate nanoplates supported on reduced graphene oxide: an effective nanocomposite for the removal of naphthalene via adsorption–photodegradation,” *ACS Omega*, vol. 6, no. 26, pp. 16783–16794, 2021.
 - [15] R. Gusain, N. Kumar, and S. S. Ray, “Recent advances in carbon nanomaterial-based adsorbents for water purification,” *Coordination Chemistry Reviews*, vol. 405, article 213111, 2020.
 - [16] A. Sridhar, M. Ponnuchamy, A. Kapoor, and S. Prabhakar, “Valorization of food waste as adsorbents for toxic dye removal from contaminated waters: a review,” *Journal of Hazardous Materials*, vol. 424, no. Part B, article 127432, 2022.
 - [17] X. Fan, L. Deng, K. Li, H. Lu, R. Wang, and W. Li, “Adsorption of malachite green in aqueous solution using sugarcane bagasse-barium carbonate composite,” *Colloid and Interface Science Communications*, vol. 44, article 100485, 2021.
 - [18] B. S. Giri, R. K. Sonwani, S. Varjani et al., “Highly efficient bio-adsorption of Malachite green using Chinese Fan-Palm Bio-char (*Livistona chinensis*),” *Chemosphere*, vol. 287, Part 3, article 132282, 2022.
 - [19] N. A. H. M. Zaidi, L. B. L. Lim, and A. Usman, “Enhancing adsorption of malachite green dye using base-modified *Artocarpus odoratissimus* leaves as adsorbents,” *Environmental Technology and Innovation*, vol. 13, pp. 211–223, 2019.
 - [20] N. C. Yildirim, M. Tanyol, N. Yildirim, O. Serdar, and S. Tatar, “Biochemical responses of *Gammarus pulex* to malachite green solutions decolorized by *Coriolus versicolor* as a biosorbent under batch adsorption conditions optimized with response surface methodology,” *Ecotoxicology and Environmental Safety*, vol. 156, pp. 41–47, 2018.
 - [21] A. S. Sartape, A. M. Mandhare, V. V. Jadhav, P. D. Raut, M. A. Anuse, and S. S. Kolekar, “Removal of malachite green dye from aqueous solution with adsorption technique using *Limonia acidissima* (wood apple) shell as low cost adsorbent,” *Arabian Journal of Chemistry*, vol. 10, pp. S3229–S3238, 2017.
 - [22] G. Sharma, S. Sharma, A. Kumar et al., “Honeycomb structured activated carbon synthesized from *Pinus roxburghii* cone as effective bioadsorbent for toxic malachite green dye,” *Journal of Water Process Engineering*, vol. 32, article 100931, 2019.
 - [23] A. Ahmad, D. Jini, D. Aravind et al., “A novel study on synthesis of egg shell based activated carbon for degradation of methylene blue via photocatalysis,” *Arabian Journal of Chemistry*, vol. 13, no. 12, pp. 8717–8722, 2020.
 - [24] B. Haddad, A. Mittal, J. Mittal et al., “Synthesis and characterization of egg shell (ES) and egg shell with membrane (ESM) modified by ionic liquids,” *Chemical Data Collections*, vol. 33, article 100717, 2021.
 - [25] P. S. Katha, Z. Ahmed, R. Alam, B. Saha, A. Acharjee, and M. S. Rahman, “Efficiency analysis of eggshell and tea waste as low cost adsorbents for Cr removal from wastewater sample,” *South African Journal of Chemical Engineering*, vol. 37, pp. 186–195, 2021.
 - [26] N. Z. Kasim, N. A. A. A. Malek, N. S. H. Anuwar, and N. H. Hamid, “Adsorptive removal of phosphate from aqueous solution using waste chicken bone and waste cockle shell,” *Materials Today: Proceedings*, vol. 31, pp. A1–A5, 2020.
 - [27] A. S. Darwish, D. I. Osman, H. A. Mohammed, and S. K. Attia, “Cuttlefish bone biowaste for production of holey aragonitic sheets and mesoporous mayenite-embedded Ag_2CO_3 nanocomposite: towards design high-performance adsorbents and visible-light photocatalyst for detoxification of dyes wastewater and waste oil recovery,” *Journal of Photochemistry and Photobiology A: Chemistry*, vol. 421, article 113523, 2021.
 - [28] M. E. Haddad, “Removal of basic fuchsin dye from water using mussel shell biomass waste as an adsorbent: equilibrium, kinetics, and thermodynamics,” *Journal of Taibah University for Science*, vol. 10, no. 5, pp. 664–674, 2016.
 - [29] V. B. Mukkanti and A. R. Tembhurkar, “Defluoridation of water using adsorbent derived from the *Labeo rohita* (rohu) fish scales waste: optimization, isotherms, kinetics, and thermodynamic study,” *Sustainable Chemistry and Pharmacy*, vol. 23, article 100520, 2021.
 - [30] J. Hu, X. Zhou, Y. Shi, X. Wang, and H. Li, “Enhancing biochar sorption properties through self-templating strategy and ultrasonic fore-modified pre-treatment: characteristic, kinetic and mechanism studies,” *Science of The Total Environment*, vol. 769, article 144574, 2021.

- [31] R. Singh and V. S. Sharanagat, "Physico-functional and structural characterization of ultrasonic-assisted chemically modified elephant foot yam starch," *International Journal of Biological Macromolecules*, vol. 164, pp. 1061–1069, 2020.
- [32] G. L. Dotto, J. M. N. Santos, I. L. Rodrigues, R. Rosa, F. A. Pavan, and E. C. Lima, "Adsorption of methylene blue by ultrasonic surface modified chitin," *Journal of Colloid and Interface Science*, vol. 446, pp. 133–140, 2015.
- [33] C. Leng, K. Sun, J. Li, and J. Jiang, "The reconstruction of char surface by oxidized quantum-size carbon dots under the ultrasonic energy to prepare modified activated carbon materials as electrodes for supercapacitors," *Journal of Alloys and Compounds*, vol. 714, pp. 443–452, 2017.
- [34] R. Zare-Dorabei, S. M. Ferdowsi, A. Barzin, and A. Tadjarodi, "Highly efficient simultaneous ultrasonic-assisted adsorption of Pb(II), Cd(II), Ni(II) and Cu (II) ions from aqueous solutions by graphene oxide modified with 2, 2'-dipyridylamine: central composite design optimization," *Ultrasonics sonochemistry*, vol. 32, pp. 265–276, 2016.
- [35] A. Saravanan, P. Senthil Kumar, D.-V. N. Vo et al., "Ultrasonic assisted agro waste biomass for rapid removal of Cd(II) ions from aquatic environment: mechanism and modelling analysis," *Chemosphere*, vol. 271, article 129484, 2021.
- [36] S. K. Low, M. C. Tan, and N. L. Chin, "Effect of ultrasound pretreatment on adsorbent in dye adsorption compared with ultrasound simultaneous adsorption," *Ultrasonics sonochemistry*, vol. 48, pp. 64–70, 2018.
- [37] R. Jothirani, P. Senthil Kumar, A. Saravanan, A. S. Narayan, and A. Dutta, "Ultrasonic modified corn pith for the sequestration of dye from aqueous solution," *Journal of Industrial and Engineering Chemistry*, vol. 39, pp. 162–175, 2016.
- [38] I. Langmuir, "The adsorption of gases on plane surfaces of glass, mica and platinum," *Journal of the American Chemical Society*, vol. 40, no. 9, pp. 1361–1403, 1918.
- [39] H. M. F. Freundlich, "Über die adsorption in Lösungen," *The Journal of Physical Chemistry*, vol. 57U, no. 1, pp. 385–470, 1907.
- [40] R. Sips, "On the structure of a catalyst surface," *The Journal of Chemical Physics*, vol. 16, no. 5, pp. 490–495, 1948.
- [41] C. Aharoni and F. C. Tompkins, "Kinetics of adsorption and desorption and the Elovich equation," in *Advances in Catalysis and Related Subjects*, D. D. Eley, H. Pines, and P. B. Weisz, Eds., pp. 21–22, Academic Press, New York, 1970.
- [42] S. Lagergren, "About the theory of so-called adsorption of soluble substances," *Kungliga Svenska Vetenskapsakademiens Handlingar*, vol. 24, pp. 1–39, 1898.
- [43] Y. S. Ho and G. McKay, "Pseudo-second order model for sorption processes," *Process Biochemistry*, vol. 34, no. 5, pp. 451–465, 1999.
- [44] M. J. D. Low, "Kinetics of chemisorption of gases on solids," *Chemical Reviews*, vol. 60, no. 3, pp. 267–312, 1960.
- [45] F. Jiang, D. M. Dinh, and Y. L. Hsieh, "Adsorption and desorption of cationic malachite green dye on cellulose nanofibril aerogels," *Carbohydrate Polymers*, vol. 173, pp. 286–294, 2017.
- [46] C. Belhajjia, A. Abid, A. Msaad, Z. Labaali, and A. Zouhri, "Synthesis, characterization and adsorption of malachite green dye using novel materiel produced from *Opuntia ficus indica*," *Materials Today: Proceedings*, vol. 37, pp. 4001–4006, 2021.
- [47] J. O. Ojediran, A. O. Dada, S. O. Aniyi, and R. O. David, "Functionalized Zea Mays Cob (FZMC) as low-cost agrowaste for effective adsorption of malachite green dyes data set," *Chemical Data Collections*, vol. 30, article 100563, 2020.
- [48] K. Buvaneswari and M. Singanan, "Removal of malachite green dye in synthetic wastewater using *Zingiber officinale* plant leaves biocarbon," *Materials Today: Proceedings*, vol. 55, pp. 274–279, 2022.
- [49] S. Vigneshwaran, P. Sirajudheen, P. Karthikeyan, and S. Meenakshi, "Fabrication of sulfur-doped biochar derived from tapioca peel waste with superior adsorption performance for the removal of malachite green and rhodamine B dyes," *Surfaces and Interfaces*, vol. 23, article 100920, 2021.
- [50] M. Ghaedi and N. Mosallanejad, "Study of competitive adsorption of malachite green and sunset yellow dyes on cadmium hydroxide nanowires loaded on activated carbon," *Journal of Industrial and Engineering Chemistry*, vol. 20, no. 3, pp. 1085–1096, 2014.
- [51] V. M. Muinde, J. M. Onyari, B. Wamalwa, and J. N. Wabomba, "Adsorption of malachite green dye from aqueous solutions using mesoporous chitosan-zinc oxide composite material," *Environmental Chemistry and Ecotoxicology*, vol. 2, pp. 115–125, 2020.
- [52] A. Rubio-Clemente, J. Gutiérrez, H. Henao, A. M. Melo, J. F. Pérez, and E. Chica, "Adsorption capacity of the biochar obtained from *Pinus patula* wood micro-gasification for the treatment of polluted water containing malachite green dye," *Journal of King Saud University-Engineering Sciences*, 2021.
- [53] H. A. Chanzu, J. M. Onyari, and P. M. Shiundu, "Brewers' spent grain in adsorption of aqueous Congo Red and malachite green dyes: batch and continuous flow systems," *Journal of Hazardous Materials*, vol. 380, article 120897, 2019.